Journal of Sciences, Islamic Republic of Iran 36(1): 61 - 67 (2025) http://jsciences.ut.ac.ir
University of Tehran, ISSN 1016-1104

Fusion Reactivity of Plasma with Anisotropic Lorentzian Distribution

F. Khoshdoun[1], M. Shahmansouri[2*]

[1] *Department of Physics, Faculty of Science, Arak University, Arak, Islamic Republic of Iran*
[2] *Department of Atomic and Molecular Physics, Faculty of Physics, Alzahra University, Tehran, Islamic Republic of Iran*

Received: 9 July 2025 / Revised: 28 September 2025 / Accepted: 8 December 2025

Abstract

Anisotropic distributions and deviations from velocity equilibrium play a crucial role in plasma physics and nuclear fusion processes. The emergence of high-energy tails in non-equilibrium distributions increases the population of energetic particles, thereby enhancing the probability of quantum tunneling and, consequently, fusion reaction rates. In this work, we investigate how the velocity-space anisotropy and deviations from the equilibrium affect the optimization of the fusion yield. Specifically, we analyze non-Maxwellian distribution models, including kappa and anisotropic kappa distributions, to evaluate their impact on fusion reactivity. Our results show that anisotropic distributions outperform isotropic ones at lower temperatures, whereas isotropic distributions dominate at higher temperatures. These findings provide new insights for the design of fusion devices and contribute to improving the efficiency of fusion processes.

Keywords: Non-Maxwellian Distributions; Kappa Distribution; Fusion Reaction Rates; Velocity Anisotropy; Magnetic Confinement.

Introduction

Investigation of non-Maxwellian energy distributions in plasma physics, particularly in the context of nuclear fusion reactions, has gained increasing attention in recent years (1-10). In classical plasma systems, Maxwell-Boltzmann (MB) distributions are often inadequate for explaining the complexities of real phenomena, where particles exhibit significant deviations from equilibrium. Such deviations are observed across a wide range of environments, from space plasmas to laboratory experiments designed for controlled fusion. To better capture these effects, various non-Maxwellian models have been proposed, including kappa distributions, bi-Maxwellian distributions, and superstatistics (6). These distributions are characterized by prominent high-energy tails, which indicate an enhanced population of energetic particles and can significantly affect nuclear fusion reaction rates. For example, non-Maxwellian distributions have been associated with increased reactivity due to the greater probability of tunneling phenomena enabled by a higher number of high-energy particles (7). Additionally, velocity-space anisotropy, introduced by mechanisms such as magnetic confinement or external heating, plays a crucial role in modifying fusion yields. At plasma temperatures lower than those corresponding to the peak of the fusion cross section, anisotropic distributions generally result in higher fusion yields compared to isotropic distributions with the same thermal energy. However, as the temperature increases,

* Corresponding Author; Tel: +989339836854; Email: m.shahmansouri@alzahra.ac.ir

isotropic distributions become dominant, highlighting the complex interplay between temperature, anisotropy, and fusion efficiency (8).

The understanding of nuclear fusion has had a profound impact on the development of plasma physics. In the following, we briefly review key historical milestones in the advancement of nuclear fusion. Arthur Eddington was the first to propose that nuclear fusion could serve as the primary energy source powering stars (11). The concept of quantum tunneling was later introduced by Gamow (12), and Atkinson and Houtermans analytically investigated nuclear fusion rates in stars (13). The first artificial nuclear disintegration was achieved by Cockcroft and Walton in 1932 (14). In 1946, Arnoux was the first to patent a fusion device, which initiated experimental research on nuclear fusion the following year (15). The stellarator concept was introduced by Spitzer (16), and the first controlled fusion experiment was conducted using Scylla (17). The first generation of tokamaks, known as T-1, was constructed in the Soviet Union (18).

Over the following decades, numerous efforts were devoted to improving fusion devices and developing related physical concepts (19-21). Among the most notable achievements, JET and ITER have played leading roles: JET produced its first plasma in 1983, and conceptual design work for ITER began in 1988. In 1991, JET performed the first deuterium–tritium fusion experiment, setting a record of 16 megawatts of fusion power. More recently, JET achieved a new record with 59 megajoules of fusion energy. Very recently, the Wendelstein 7-X produced plasma with gigajoule-scale energy, while KSTAR set a record of 102 seconds of stable plasma at 10^8 ℃ in 2024 (21).

Recent research has increasingly focused on the effects of velocity-space deviations in plasmas and their influence on nuclear fusion yields. Kolmes *et al*., (13) demonstrated that velocity deviations in plasmas can significantly enhance fusion reactions, particularly at lower temperatures. They suggested that non-isotropic distributions provide superior performance at low temperatures, although this advantage diminishes as the temperature increases. Ourabah (19) examined reaction rates in systems near local equilibrium and showed that non-Maxwellian distributions can increase fusion yields, identifying specific conditions under which such distributions strongly enhance fusion activity. Furthermore, Onofrio and Sundaram (18) investigated the role of particular energy distributions and their applications in fusion devices. Their work indicated that non-Maxwellian energy distributions can improve fusion performance under certain conditions, especially in modern devices designed to exploit such distributions. Recently, Xie (26) introduced an efficient computational framework for solving plasma waves with arbitrary energy distributions, which also covers the analysis of kappa and anisotropic distributions. This method provides a useful tool for more accurate investigations of instabilities and fusion reactions in non-Maxwellian environments. Nerney (27) recently modeled anisotropic Maxwellian and Kappa distributions in Io's plasma torus, showing that distribution choice and temperature anisotropy strongly affect plasma density and temperature profiles.

The present study builds on historical advancements and recent research on non-equilibrium and anisotropic distributions-arising from external heating or magnetic confinement-to investigate how statistical particle distributions affect reaction rates in anisotropic plasma systems. The findings are expected to provide a new perspective on optimizing fusion processes and to contribute to a deeper understanding of energy transfer in complex plasma environments. This study is presented as a research article; the background material included in the introduction is intentionally concise and serves only to provide context for the new derivations and numerical analysis. In this work, we extend the standard anisotropic-kappa framework to derive new reactivity expressions by incorporating the anisotropic distribution into the fusion cross-section integral and explicitly performing the angular integration. To the best of our knowledge, this explicit angular-integral formulation for the anisotropic kappa distribution has not been reported previously. Our numerical analysis further explores how anisotropy and suprathermal tails influence reactivity across the relevant parameter ranges.

Materials and Methods

Anisotropic Kappa Distribution

The anisotropic kappa distribution is a version of the kappa distribution used in situations where the characteristics of non-equilibrium systems are distributed differently across various spatial directions. In plasma physics and astrophysics, plasma systems often exhibit anisotropic properties, meaning physical properties (e.g., temperature and density) vary across different directions (22,23).

The anisotropic kappa distribution is particularly useful for modeling such systems. The formula for the anisotropic kappa distribution in velocity coordinates $v = (v_\perp, v_\parallel)$ is as follows (24):

$$f(v) = \frac{n\Gamma(\kappa+1)}{\pi^{3/2}\theta_\perp^2\theta_\parallel\kappa^{3/2}\Gamma(\kappa-\frac{1}{2})}\left[1+\frac{1}{\kappa}\left(\frac{v_\perp^2}{\theta_\perp^2}+\frac{v_\parallel^2}{\theta_\parallel^2}\right)\right]^{-(\kappa+1)} \quad (1)$$

where n denotes the particle number density, κ is the

spectral index governing the suprathermal tail of the distribution, $\theta_\perp$ and $\theta_\parallel$ are the effective temperature parameters perpendicular and parallel to the magnetic field (or reference axis), respectively, also $v_\perp$ and, $v_\parallel$ are the corresponding velocity components. In the limit $\kappa \to \infty$, the anisotropic kappa distribution reduces to the bi-Maxwellian distribution.

In plasma physics, particularly in the analysis of particle motion in strong magnetic fields, it is common to separate the perpendicular and parallel energies with respect to the field as $E_\perp = \frac{1}{2}mv_\perp^2$ and $E_\parallel = \frac{1}{2}mv_\parallel^2$. This separation naturally allows the distribution to be expressed in terms of perpendicular and parallel energy coordinates, as follows (23):

$$f(E_\perp, E_\parallel) = \frac{n}{\pi^{3/2}\theta_\perp^2\theta_\parallel\kappa^{3/2}}\frac{\Gamma(\kappa+1)}{\Gamma(\kappa-1/2)}\left[1+\frac{\beta}{\kappa}(\beta_\perp E_\perp + \beta_\parallel E_\parallel)\right]^{-(\kappa+1)} \quad (2)$$

In Eq. (2), the parameters $\beta_\perp = 1/\beta\theta_\perp$ and $\beta_\parallel = 1/\beta\theta_\parallel$ represent the inverse effective temperatures in the perpendicular and parallel directions, respectively; and β as a normalization factor is given by $0.1(keV)^{-1}$ refers to a typical value of deuterium-tritium reaction (28).

To obtain the distribution function as a function of the total kinetic energy, one must integrate the velocity-space distribution over all angles in spherical coordinates. For an anisotropic, axis- preferred distribution (e.g., aligned with the magnetic field vector), it is convenient to adopt spherical coordinates, with $v_\parallel = vcos\theta$, $v_\perp = vsin\theta$ and $E = \frac{1}{2}mv^2$. The number of particles with energy between E and $E + dE$ is then given by the following integral expression (23):

$$f(E) = 4\pi \int f(v)\delta\left(\frac{1}{2}mv^2 - E\right)v^2 dv \quad (3)$$

In Eq. (3), $f(E)$ denotes the single-particle energy distribution obtained by integrating the velocity-space formulation. The angle θ is the polar angle measured relative to the magnetic-field (parallel) direction. This transformation ensures that the anisotropic kappa distribution can be expressed consistently in terms of the total particle energy. For normalization, the integration is restricted to the region where $E = \frac{1}{2}mv^2$. In spherical velocity coordinates (relative to the parallel axis), the volume element is $d^3v = v^2 sin\theta dv d\varphi d\theta$. Assuming azimuthal symmetry about φ (rotation around the parallel axis), the integral over φ contributes only a factor of 2π, consistent with the azimuth-integrated forms.

The result (without delving into the full details of integration) is as follows (23):

$$f(E) = \frac{\Gamma(\kappa+1)}{\kappa^{3/2}\Gamma(\kappa-\frac{1}{2})}\underbrace{\frac{n}{\pi^{3/2}\theta_\perp^2\theta_\parallel}}\left(\frac{E}{m}\right)^{\frac{3}{2}}\int_0^\pi\left[1+\frac{\beta E}{\kappa}(\beta_\perp sin^2\theta + \beta_\parallel cos^2\theta)\right]^{-(\kappa+1)} sin\theta d\theta \quad (4)$$

In Eq. (4), $f(E)$ denotes the azimuthally integrated anisotropic kappa distribution expressed as a function of the total particle energy. This compact form, obtained by carrying out the angular integrations, provides a convenient representation of the energy distribution for subsequent evaluation of fusion reactivity. The resulting $f(E)$ is fully consistent with the azimuth-independent anisotropic-kappa formulation.

In the following, we derive an explicit expression for the fusion reactivity in anisotropic, non-thermal plasmas. The tunneling cross section, formulated in terms of the anisotropic kappa velocity distribution $f(v)$, takes the form (25):

$$\langle\sigma v\rangle = \int_0^\infty\int_0^\pi\left[1+\frac{\beta E}{\kappa}(\beta_\perp sin^2\theta + \beta_\parallel cos^2\theta)\right]^{-(\kappa+1)} T(E)E^{-1/2}\, d\theta dE \quad (5)$$

In Eqs. (5)-(8), $\langle\sigma v\rangle$ denotes the fusion reactivity, defined as the velocity-averaged product of the fusion cross section $\sigma(E)$ and the relative velocity v of the reacting particles. Here, $\sigma(E)$ is the energy-dependent nuclear fusion cross section, while v represents the relative speed between the interacting nuclei. This quantity serves as the fundamental link between microscopic nuclear properties and macroscopic reaction rates in plasmas.

The angular integration over $d\theta$ explicitly incorporates anisotropy arising from temperature differences in the perpendicular and parallel directions. The transmission coefficient $T(E)$ is typically modeled with either exponential or power-law dependence:

$$T(E) = \begin{cases}\left(\frac{E}{E_0}\right)^\alpha & for\ E < E_0, \\ 1 & for\ E > E_0.\end{cases} \quad (6)$$

where E_0 refers to threshold energy that serves as a modeling parameter that defines the boundary between the gradual growth region and saturation region of the tunneling coefficient; α represents role of a convexity parameter varies between 0 and ∞, as for $E < E_0$, we have $T(E)$ concave (convex) if α < 1 (if α > 1). This formulation incorporates the effect of anisotropic temperatures ($\beta_\perp$ and $\beta_\parallel$) on reactivity calculations.

Reactivity ($\delta R_{a\kappa}$) of fusion

To quantify the enhancement of reactivity in the anisotropic kappa distribution relative to the Maxwell–Boltzmann case, we evaluate and compare the reactivity

within two distinct frameworks, as follows:

$$\delta R_{a\kappa} = \langle \sigma v \rangle_{a\kappa} - \langle \sigma v \rangle_{MB} \quad (7)$$

Substituting the anisotropic kappa distribution from Eq. (4) into δR_κ we obtain:

$$\delta R_{a\kappa} = \int_0^\infty \int_0^\pi \left(\left[1 + \frac{2\beta E}{\kappa} (sin^2\phi\, \beta_\perp + cos^2\phi\, \beta_\parallel) \right]^{-(\kappa+1)} - p_{MB}(E) \right) T(E) E^{-1/2}\, d\phi dE \quad (8)$$

where:

$$p_{MB}(E) = \sqrt{\frac{\beta}{4\pi}} E^{-1/2} \exp(-\beta E) \quad (9)$$

The angular part of integration in Eq. (8) is evaluated using the Gauss–Kronrod algorithm to compute single-variable integrals (8).

Results and Discussion

To investigate the influence of anisotropy and deviations from equilibrium, we numerically analyze the dependence of fusion reactivity on the anisotropic parameters ($\beta_\perp, \beta_\parallel$) and the spectral index κ. Figure 1, illustrates pronounced differences between the anisotropic and standard kappa distributions. At high energies (above $\beta E = 10^1$), the particle density in the anisotropic case is significantly reduced; for instance, at $\beta E = 10^2$, the value of $f(E)$ is nearly an order of magnitude lower than in the standard kappa distribution. This suppression of suprathermal tails enhances plasma stability and reduces energy losses. Here, plasma stability refers specifically to kinetic regimes where suprathermal particles do not strongly drive wave–particle instabilities and transport-related energy losses remain minimized. More precisely, stability is defined as the ability of the anisotropic kappa distribution to remain self-consistent without exciting mirror, whistler, or firehose modes, while simultaneously reducing collisional and turbulent losses. Our numerical results confirm this definition; as the parameter ranges that enhance reactivity (low κ and moderate $T_\perp/T_\parallel$) coincide with conditions where suprathermal particles are less destabilizing.

At low energies (below $\beta E = 10^{-1}$), the anisotropic distribution exhibits higher particle densities. For example, at $\beta E = 10^{-2}$, $f(E)$ is nearly an order of magnitude greater than in the standard kappa distribution. This enhancement is particularly favorable for fusion reactions at low temperatures. In the intermediate regime ($10^{-1} < \beta E < 10^1$), the anisotropic kappa distribution is more compressed and has a shallower slope compared to the standard case, highlighting anisotropy as a potential mechanism for controlling energy distribution in plasmas.

The parameters $\beta_\parallel$ and $\beta_\perp$ independently regulate transverse and longitudinal energies. Larger values $\beta_\parallel =$

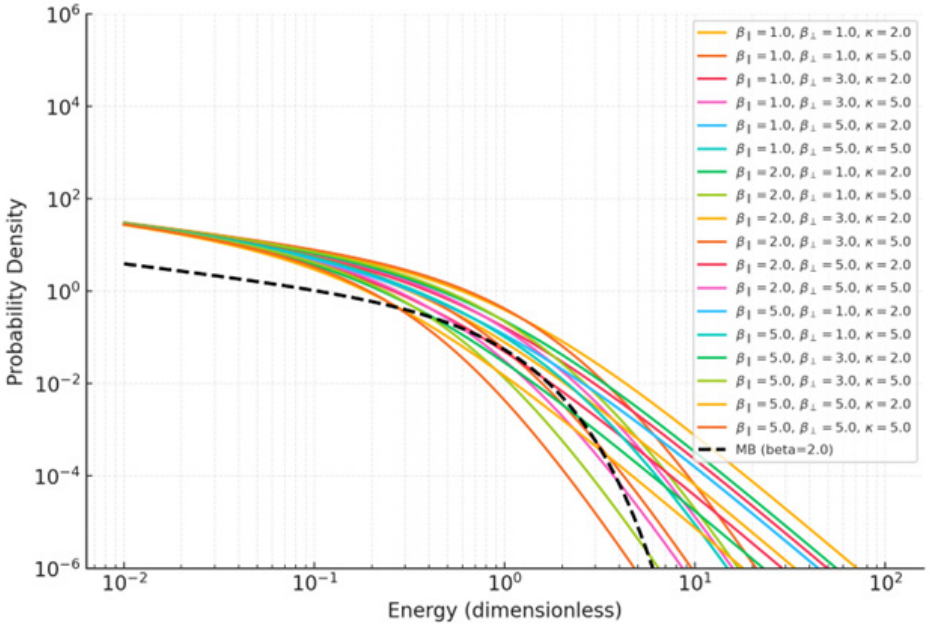

Figure 1. Anisotropic Kappa distributions for the various values of β and κ, as a function of energy. Colored lines indicate different values of $\beta_\parallel$ and $\beta_\perp$. The dashed black line represents the Maxwell-Boltzmann distribution for $\beta = 2.0$ as a reference.

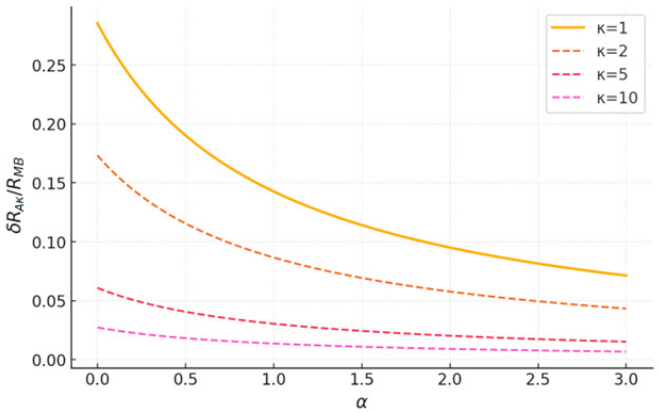

Figure 2. Variation of $\delta R_{A\kappa}/R_{MB}$ as a function of α for different values of spectral parameter κ.

5.0 and $\beta_\perp = 5.0$ shift the anisotropic kappa distribution closer to the Maxwell–Boltzmann (MB) form, although the extended high-energy tails characteristic of kappa distributions remain. The dashed black curve in Figure 1 represents the MB distribution for $\beta = 2.0$. At high energies ($\beta E > 10^1$), this curve lies well below the kappa distributions and lacks suprathermal tails, but at intermediate and low energies, the anisotropic kappa distribution converges toward *MB*. In summary, the anisotropic kappa distribution reduces high-energy tails while increasing particle densities at low energies, thereby providing a more favorable balance than the standard kappa distribution. These features enhance plasma stability, lower energy losses, and optimize conditions for fusion reactivity, making the anisotropic kappa framework particularly attractive for next-generation plasma confinement systems.

Figure 2 examines the variation of $\delta R_{a\kappa}/R_{MB}$ with α. It can be seen that as α increases, the reactivity decreases. For $\kappa = 1$, the ratio drops from approximately 0.25 at $\alpha = 0$ to 0.05 at $\alpha = 3$. For $\kappa = 2$, the decline is from about 0.15 to 0.03, while for $\kappa = 5$ and $\kappa = 10$ the initial values (≈ 0.08 and ≈ 0.05, respectively) decrease to 0.015 and 0.01 at $\alpha = 3$. These results show that small κ values ($\mathrm{e.g.}, \kappa = 2$) yield higher reactivity at low energies and small α, but fall off more steeply with increasing α. In contrast, larger κ values ($\mathrm{e.g.}, \kappa = 10$) exhibit more stable behavior and perform better at higher temperatures. Increasing $\beta_\perp$ generally enhances overall reactivity, particularly at small κ. This analysis underscores the importance of optimizing κ, α, and $\beta_\perp$ to maximize reactivity under diverse plasma conditions. To compute the reactivities the experimental cross sections parametrized in Ref. (28) has been used by integrating the reactivity over the energy validated intervals.

Figure 3 further illustrates the dependence of relative reactivity ($\delta R_{a\kappa}/R_{MB}$) on α for different $\beta_\parallel$ values. With $\beta_\parallel = 5.0$, the reactivity at $\alpha = 0$ is about 2.5 for $\kappa = 2$ and 1.5 for $\kappa = 10$. As α increases, the values decrease to ≈ 0.5 and ≈ 0.8, respectively, at $\alpha = 2.5$. Thus, small κ yields higher reactivity at low energies but declines more steeply. For $\beta_\parallel = 10$, the reactivity rises: at $\alpha = 0$, the values are ≈ 3.5 for $\kappa = 2$ and ≈ 1.8 for $\kappa = 10$. By $\alpha = 2.5$, they reduce to ≈ 1.0 and ≈ 0.9, respectively. This trend confirms that smaller κ values perform better at low energies but are more sensitive to increasing α. For $\beta_\parallel = 20$, the reactivity at $\alpha = 0$ reaches ≈ 5.5 for $\kappa = 2$ and ≈ 2.2 for $\kappa = 10$. As α increases, the values decrease to ≈ 1.5 and ≈ 1.2, respectively. Again, $\kappa = 2$ delivers stronger performance at low energies but declines more sharply than $\kappa = 10$.

Conclusion

This study highlights the critical role of non-Maxwellian energy distributions and anisotropy in plasma physics, with particular emphasis on kappa distributions and their comparison to the Maxwell–Boltzmann (MB) case. The main conclusions are as follows:

In anisotropic plasmas, temperature differences between parallel ($\beta_\parallel$) and perpendicular ($\beta_\perp$) directions strongly shape the particle energy distribution.

At low α, the contribution of suprathermal particles to fusion is negligible, and the fusion rate ($R_{A\kappa}$) is nearly identical to the MB result (R_{MB}).

As α increases, the extended high-energy tails of kappa distributions substantially enhance tunneling probabilities and fusion rates, particularly for small κ.

When $\beta_\parallel > \beta_\perp$, anisotropy further amplifies the role of high-energy particles in the perpendicular direction,

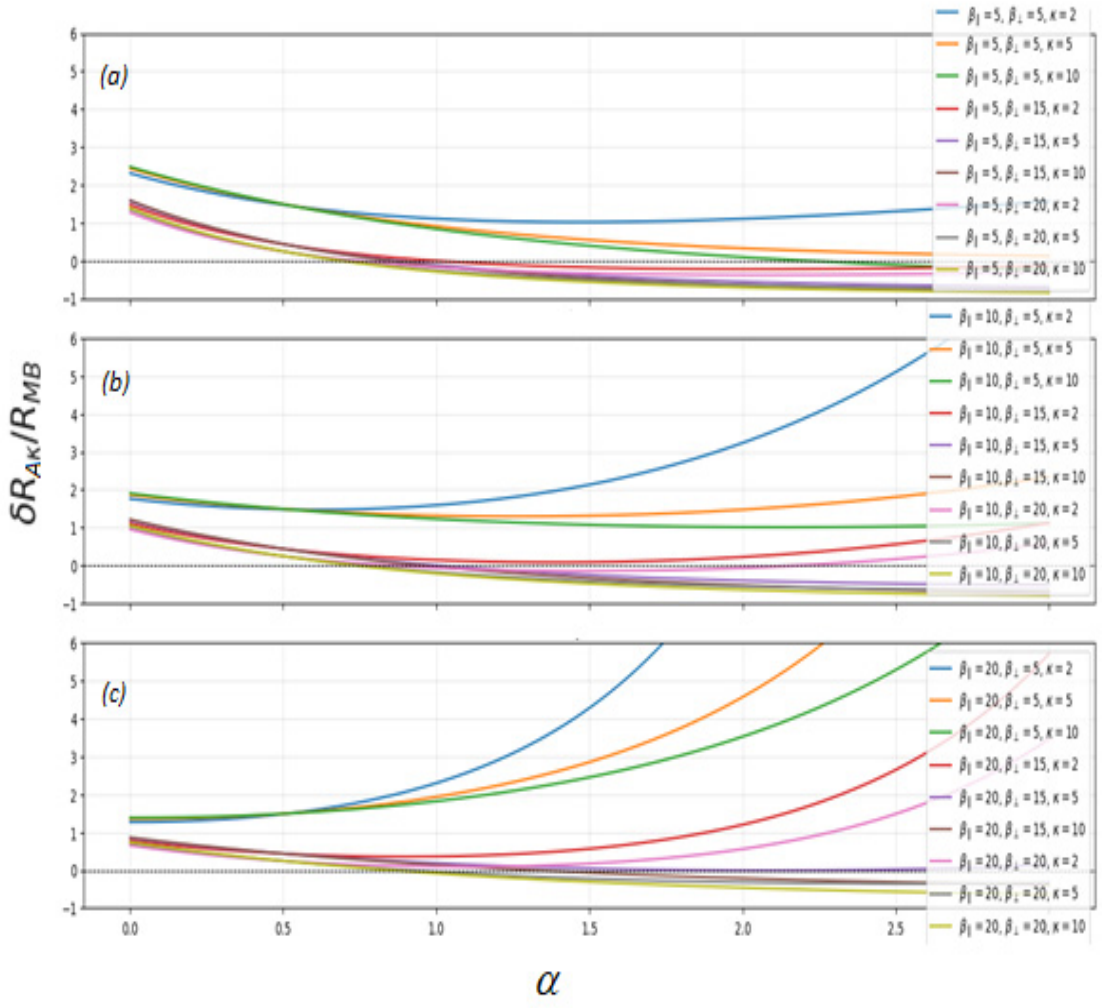

Figure 3. Comparison of the variation of $\delta R_{\kappa}/R_{MB}$ for different values of κ and $\beta_{\perp}$ across the three values of (a) $\beta_{\parallel}=5$, (b) $\beta_{\parallel}=10$ and (c) $\beta_{\parallel}=20$.

yielding higher fusion rates compared to MB.

The temperature ratio determines the dominant contribution to the overall fusion rate; increasing $T_{\perp}$ under suitable conditions significantly boosts reactivity.

Higher α values magnify sensitivity to high-energy particles, underscoring the advantage of kappa distributions for improving fusion efficiency.

Overall, kappa distributions-together with controlled anisotropy-offer far greater flexibility than MB in modeling the high-temperature plasmas. They not only enhance fusion rates but also enable more effective use of energetic particles under tailored confinement conditions. In magnetic confinement systems, external heating and temperature anisotropy can be exploited to maximize yields, while in inertial confinement, engineered plasma environments benefit from non-Maxwellian statistics.

By fine-tuning key parameters (κ , α , β), fusion efficiency can be significantly improved. These findings point toward practical pathways for optimizing confinement strategies and advancing the development of sustainable and clean nuclear fusion energy.

References

1. Luo L, Ma M, Yang Y, Zhao H. Case Report: Genetic 1. Borhanian J, Shahmansouri M. Spherical electron acoustic solitary waves in plasma with suprathermal

electrons. Astrophys Space Sci. 2012;342:401.
2. Shahmansouri M, Borhanian J. Spherical Kadomtsev–Petviashvili solitons in a suprathermal complex plasma. Commun Theor Phys. 2013;60:227.
3. Shahmansouri M, Tribeche M. Large amplitude dust ion acoustic solitons and double layers in dusty plasmas with ion streaming and high-energy tail electron distribution. Commun Theor Phys. 2014;61:377.
4. Ainejad H, Mahdavi M, Shahmansouri M. Effects of superthermal electrons and negatively (positively) charged dust grains on dust-ion acoustic wave modulation. Eur Phys J Plus. 2014;129(5):99.
5. Shahmansouri M, Tribeche M. Dust acoustic shock waves in suprathermal dusty plasma in the presence of ion streaming with dust charge fluctuations. Astrophys. Space Sci. 2013;343:251.
6. Bethe HA. Energy production in stars. Phys Rev. 1939;55(5):434–56. doi:10.1103/PhysRev.55.434.
7. Bethe HA, Critchfield CL. The formation of deuterons by proton combination. Phys Rev. 1938;54(4):248–54. doi:10.1103/physrev.54.248.
8. Calió F, Gautschi W, Marchetti E. On computing Gauss-Kronrod quadrature formulae. Math Comput. 1986;47(176):639–50.
9. Crilly AJ, Appelbe BD, Mannion OM, Taitano W, Chittenden JP. Constraints on ion velocity distributions from fusion product spectroscopy. Nucl Fusion. 2022;62(12):126015.
10. Daniel HP, Moya PS, Zenteno-Quinteros B, Colmenares GA. Magnetic spectra comparison for kappa-distributed whistler electron fluctuations. Astrophys J. 2024;970(1):132.
11. Eddington AS. The internal constitution of the stars. Science. 1920;52(1341):233–40.
12. Hendry J, Lawson J. Fusion research in the UK 1945–1960. AEA Technology; 1993.
13. Kolmes EJ, Mlodik ME, Fisch NJ. Fusion yield of plasma with velocity-space anisotropy at constant energy. Princeton University, Department of Astrophysical Sciences; 2021.
14. Li K, Liu ZY, Yao YL, Zhao ZH, Dong C, Li D, et al. Modification of the fusion energy gain factor in magnetic confinement fusion due to plasma temperature anisotropy. Nucl Fusion. 2022;62(12):126015.
15. Miyamoto K. Plasma physics for controlled fusion. Berlin Heidelberg: Springer-Verlag; 2016.
16. Yang S, et al. Tailoring tokamak error fields to control plasma instabilities and transport. Nat Commun. 2024;15:1275. doi:10.1038/s41467-024-45454-1.
17. Nimtz G, Clegg B. Compendium of quantum physics. Berlin: Springer; 2009. p. 799–802. ISBN 978-3-540-70622-9.
18. Onofrio R, Sundaram B. Relationship between nonlinearities and thermalization in classical open systems: The role of the interaction range. Phys Rev E. 2024;101(1):123–34.
19. Ourabah K. Reaction rates in quasiequilibrium states. Phys Rev E. 2024;111:034115.
20. Rebut P-H. The JET preliminary tritium experiment. Plasma Phys Control Fusion. 1992;34(13):1749–58. doi:10.1088/0741-3335/34/13/002.
21. Smirnov VP. Tokamak foundation in USSR/Russia 1950–1990. Nucl Fusion. 2009;50(1):014003. doi:10.1088/0029-5515/50/1/014003.
22. Squarer BI, Presilla C, Onofrio R. Enhancement of fusion reactivities using non-Maxwellian energy distributions. Phys Rev E. 2024;101(1):123–34.
23. Livadiotis G, Nicolaou G, Allegrini F. Anisotropic kappa distributions. I. Formulation based on particle correlations. Astrophys J. 2021;253:16.
24. Shahmansouri M, Lee MJ, Jung YD. Anisotropic temperature effects on Landau damping in Kappa-Maxwellian astrophysical plasmas. Astropart Phys. 2020;130:102449. doi:10.1016/j.astropartphys.2020.102449.
25. Atkinson RdE, Houtermans FG. Zur Frage der Aufbaumöglichkeit der Elemente in Sternen. Z Phys. 1929;54(9–10):656–65. doi:10.1007/BF01341595.
26. Xie H. Efficient framework for solving plasma waves with arbitrary distributions. Phys. Plasmas 2025;32:060702.
27. Nerney EG. Diffusive equilibrium: Modeling anisotropic Maxwellian and Kappa field line distributions in Io's plasma torus using multi-fluid and kinetic approaches. J Geophys Res Space Phys. 2025. doi:10.22541/essoar.175009109.95959011/v1
28. Bosch HS, Hale, GM. Improved formulas for fusion cross-sections and thermal reactivities. Nucl. Fusion 1992;32:611.